Italian Journal of Food Science, 2026; 38 (1): 321–335

Micellar extraction of lipophilic metabolites from turmeric

Misael Cortés-Rodríguez[1]*, Valentina Quintero-Gómez[2], Óscar Hernán Giraldo-Osorio[3]

[1]Functional Foods Research Group, Department of Agricultural and Food Engineering, Faculty of Agricultural Sciences, Universidad Nacional de Colombia, Medellín, Colombia; [2]Faculty of Sciences, Universidad Nacional de Colombia, Medellín, Colombia; [3]Grupo de Investigación de Procesos Químicos, Catalíticos y Biotecnológicos, Departamento de Física y Química, Facultad de Ciencias Exactas y Naturales, Universidad Nacional de Colombia, Manizales, Colombia

***Corresponding Author:** Misael Cortés-Rodríguez, Functional Foods Research Group, Department of Agricultural and Food Engineering, Faculty of Agricultural Sciences, Universidad Nacional de Colombia, Medellín, Colombia. Email: mcortesro@unal.edu.co

Academic Editor: Prof. Antonietta Baiano – University of Foggia, Italy

Received: 24 September 2025; Accepted: 17 November 2025; Published: 3 January 2026

ORIGINAL ARTICLE

Abstract

This work aimed to optimize the micellar extraction of bioactive compounds from turmeric, using sodium oleate as surfactant. Response surface methodology was employed, considering the independent variables: mass ratio of turmeric/micellar solution (MS) of sodium oleate (MS_{SO}), surfactant concentration and extraction time (t_E). The turmeric/MS_{SO} ratio and surfactant mainly affected the process. The optimal conditions were as follows: turmeric/MS_{SO} = 0.01, surfactant = 1.525% and t_E = 6.6 min; and the dependent variables: TPC = 181.6 ± 3.0 mg gallic acid equivalent/g turmeric dry basis (db); $DPPH^{\bullet}$ = 50.6 ± 1.1 mg Trolox equivalent (TE)/g turmeric db; $ABTS^{\bullet+}$ = 142.7 ± 7.9 mg TE/g turmeric db; curcumin = 11.6 mg/g turmeric db. Micellar extraction is a sustainable, economical, and simple process compared to the conventional ethanol method.

Keywords: bioactive compounds; *Curcuma longa* L.; curcumin; micellar extraction; sodium oleate

Introduction

The turmeric rhizome (*Curcuma longa* L.) has been used since ancient times for medicinal, cultural, and culinary purposes (Esparza, 2021). Its high content of bioactive compounds, primarily curcuminoids, imparts antioxidant, anti-inflammatory, antimutagenic, chemopreventive, antiangiogenic, hepatoprotective, and antibiotic properties, among others (Fuloria *et al*., 2022; Papayrata *et al*., 2024; Wu *et al*., 2024).

Various methodologies have been employed to extract curcuminoids; however, challenges persist due to their low water solubility, chemical instability at neutral and alkaline pH, and photosensitivity (Fuloria *et al*., 2022). Conventional extraction methods, which typically involve toxic solvents, can yield high quantities but require long processing times, high energy consumption, and are not environmentally sustainable (Ahmed *et al*., 2023; Gökdemir *et al*., 2020). Alternatively, nonconventional technologies have been explored, including supercritical fluids (Sharma *et al*., 2023), ultrasound (Patil and Rathod, 2020), microwaves (Doldolova *et al*., 2021), enzyme-assisted extraction (Le-Tan and Jaeger, 2022), deep eutectic solvents (Doldolova *et al*., 2021), and ionic liquids (Gökdemir *et al*., 2020). While these methods can achieve yields comparable to or better than conventional techniques, they still involve significant time and cost.

Micellar extraction, also known as surfactant-mediated extraction, has demonstrated high efficiency, short processing times, and low environmental impact when applied to plant matrices (Azooz *et al*., 2021; Śliwa and Śliwa, 2021). However, its application to turmeric rhizomes has been limited. The micellar extraction process begins with the simultaneous micellization of the surfactant (micelle formation at the critical micellar concentration [CMC]) and the solubilization of bioactive compounds. In an aqueous medium, the hydrophobic part of the surfactant (alkyl chains) orients toward the micelle's interior. In contrast, the hydrophilic part moves toward the surrounding aqueous solution (Śliwa and Śliwa, 2021). Micelles can aggregate into various structures (e.g., spherical micelles, worm-like micelles, vesicles, cubosomes), depending on the structural characteristics of the surfactant, pH, temperature, and other factors (Suga *et al*., 2016).

Extraction efficiency is influenced by the spatial configuration of the surfactant; specifically, the size and surface area of the micelle (Othman *et al*., 2019; Suliman *et al*., 2022; Yamini *et al*., 2020); the structure of the bioactive compounds (Śliwa and Śliwa, 2020); the length of the aliphatic chain of the surfactant (Vinarov *et al*., 2018); the use of ionic or nonionic surfactants and their combinations (Zarei, 2009); and the surfactant's hydrophilic–lipophilic balance (Khani *et al*., 2019). Micelles exist in dynamic equilibrium with monomers in the aqueous phase, facilitating interactions between the bioactive compounds and the surfactant (Śliwa and Śliwa, 2021).

Solubilization primarily occurs through hydrophobic interactions between bioactive compounds and surfactant molecules (Śliwa and Śliwa, 2020). According to Śliwa and Śliwa (2020), polyphenol solubilization within micelles occurs in three stages: (1) slow diffusion of bioactive compounds to the micellar surface; (2) absorption; and (3) rapid incorporation into the micelle structure. The location of bioactive compounds within the micelle depends on their hydrophobicity: highly hydrophobic compounds migrate toward the nucleus; moderately hydrophobic bioactive compounds reside between the aliphatic chains and the polar regions; and hydrophilic molecules remain on the micellar surface (Rangel-Yagui *et al*., 2005). Additional factors influencing simultaneous solubilization and micellar extraction include hydrogen bonding and electrostatic interactions (Azooz *et al*., 2021; Śliwa *et al*., 2019).

Sodium oleate in aqueous solution exhibits a low Krafft temperature, indicating that micelle formation and, consequently, micellar extraction can occur without heating (He *et al*., 2019). Furthermore, it inhibits enzymatic pathways responsible for curcuminoid conjugation, thereby enhancing the bioavailability of curcuminoids (Dong *et al*., 2017). Some researchers report high efficiency, with phenol extraction yields of up to 82.0% from wastewater (Zhang *et al*., 2023).

In this context, the present study aimed to experimentally optimize the micellar extraction process for extracting bioactive compounds from turmeric using sodium oleate as surfactant, and to compare its performance with that of conventional ethanol-based extraction.

Materials and Methods

Materials and reagents

Turmeric rhizomes cultivated in La Julia, located in Montenegro, Quindío, Colombia, were used in this study. The micellar extract of turmeric was prepared using a mixture consisting of oleic acid (Sigma-Aldrich, St. Louis, MO, USA), sodium hydroxide (Panreac, Spain), glacial acetic acid (Scharlau, Spain), and deionized water.

Micellar extraction

The micellar extract was prepared following the methodology described by Śliwa and Śliwa (2020), with modifications. Initially, the micellar solution (MS) of sodium oleate (MS_{SO}) was prepared using the required amount of water, based on the turmeric/MSso mass ratio defined for each experiment. This solution was then mixed with the crushed turmeric using a Silverson L5M homogenizer (Silverson Machines Ltd., UK), equipped with a standard emulsifying mesh head, operating at 5000 rpm for the extraction times (t_E) specified in the experimental design.

Subsequently, the mixture was filtered through a cloth to remove unsolubilized lignocellulosic residue. The resulting supernatant was adjusted to a pH between 6 and 7 with glacial acetic acid and stored at 5°C for characterization.

The micellar extraction process was evaluated using response surface methodology with a face-centered central composite design ($\alpha = 1$), comprising 19 experiments. The independent variables considered were: turmeric/MS_{SO} ratio (0.01–0.05 g/g); surfactant concentration (0.070–1.525%); and t_E (5–15 min). The dependent variables were: total phenolic content (TPC); antioxidant capacity (DPPH$^{\bullet}$ and ABTS$^{\bullet+}$); curcumin (CUR); particle size (φ); and zeta potential (ζ).

The dependent variables were modelled using a second-order polynomial model (Equation 1),

where *Y* represents the dependent variable and A, B, and C are the independent variables, β_0 is the model constant, β_A, β_B, and β_C are the linear coefficients, β_{AA}, β_{BB}, and β_{CC} represent the quadratic coefficients, and β_{AB}, β_{AC}, and β_{BC} are the linear interaction coefficients of the independent variables:

$$Y = \beta_0+\beta_A A + \beta_B B + \beta_C C + \beta_{AB} AB + \beta_{AC} AC + \beta_{BC} BC + \beta_{AA} A^2 + \beta_{BB} B^2 + \beta_{CC} C^2 \quad (1)$$

A multiresponse experimental optimization was also conducted to determine the independent variables that ensure the physicochemical stability of the micellar extract, and to maximize the TPC, DPPH•, $ABTS^{\bullet+}$, and CUR content. The models were validated, and the mean relative error (MRE) was calculated using Equation 2. Experimental values were obtained from three replicate experiments under optimal conditions.

$$MRE = \left| \frac{\text{Model value} - \text{Experimental value}}{\text{valueModel value}} \right| \times 100 \quad (2)$$

Conventional extraction

Micellar extraction was performed following the methodology described by Yang *et al*. (2020), using 80% ethanol (Sigma-Aldrich, USA). Initially, 2 g of crushed turmeric and 50 mL of 80% ethanol were placed in a plastic-covered Erlenmeyer flask and incubated for 60 min in a water bath maintained at 35°C. The flask was mounted on a horizontal shaking device (model SV 29/45, Memmert, Germany) operating at 105 oscillations/min. Subsequently, the mixture was centrifuged, and the supernatant was collected and stored at 5°C for characterization.

Extract characterization

Total phenolic content was determined using the Folin–Ciocalteu method, following the modified procedure of Pandey *et al*. (2021). In an amber container, 50 mL of the sample was diluted with 950 mL of ethanol. Then, 50 mL of the diluted sample was mixed with 800 mL of distilled water and 100 mL of 20% w/v Na_2CO_3 solution and left to stand in the dark for 5 min. Subsequently, 50 mL of 1 N Folin–Ciocalteu reagent (Sigma-Aldrich, St. Louis, MO, USA) was added, stirred, and allowed to react in the dark for 2 h. The absorbance was then measured at λ = 765 nm. TPC was expressed as mg gallic acid equivalent (GAE)/g turmeric dry basis (db), based on a calibration curve that related the absorbance to the concentration of a gallic acid standard (Sigma-Aldrich, USA), with the equation: Absorbance = 0.0033 (GAE concentration) – 0.1079 (R^2 = 0.991).

The antioxidant capacity was determined using the $ABTS^{\bullet+}$ and DPPH• methods. For $ABTS^{\bullet+}$, the modified methodology of Hemlata *et al*. (2020) was followed. A stock solution of the $ABTS^{\bullet+}$ radical was prepared by mixing ABTS reagent (Sigma-Aldrich, USA) with potassium persulfate (J.T. Baker, Madrid, Spain). The working solution was obtained by diluting an aliquot of the stock solution in ethanol until an absorbance of 0.700 ± 0.002 was reached. A mixture of 100 mL of sample and 900 mL of ethanol was prepared separately. From this mixture, 50 mL was combined with 950 mL of the working solution and left to stand in the dark for 7 min. The absorbance was then measured at λ = 734 nm.

For the DPPH• assay, a modified version of the method by Hemlata *et al*. (2020) was used. A stock solution of the DPPH• radical was prepared by dissolving DPPH reagent (Sigma-Aldrich, USA) in ethanol until an absorbance of 0.700 ± 0.002 was reached. A separate mixture of 200 mL of sample and 800 mL of ethanol was prepared, from which 50 mL was added to 1000 mL of the DPPH• solution. The final mixture was left to stand in the dark for 30 min, and the absorbance was measured at λ = 517 nm.

Results from both assays were expressed as mg Trolox equivalent (TE)/g turmeric db, where calibration curves were previously constructed, recording the absorbance versus the concentration of Trolox standards (Sigma-Aldrich, USA): $ABTS^{\bullet+}$ (Inhibition (%) = 0.151(TE concentration) – 1.431, R^2 = 0.9989) and DPPH• (Inhibition (%) = 0.222(TE concentration) – 1.616, R^2 = 0.994).

Curcumin was quantified using the methodology described by Yusuf *et al*. (2021), employing a Shimadzu 20A high-performance liquid chromatograph equipped with a DGU 20A5 degasser, SPD–M20A diode array detector, RID-10A refractive index detector, LC-20AD autosampler, and CTO-10A oven. A Luna C18 column (5 µm, 250 × 4.6 mm) and an AJO 4287 precolumn (Phenomenex, Torrance, CA, USA) were used. An isocratic method was employed, utilizing a mobile phase composed of a 50:50 (v/v) mixture of 1% w/v aqueous acetic acid and gradient-grade acetonitrile (Merck KGaA, Germany). Initially, 100 µL of the sample was dissolved in 900 µL of the mobile phase, shaken, and filtered through a 0.45 µm polyvinylidene fluoride syringe filter (Whatman, UK). Finally, 20 µL of the resulting solution was injected into the chromatograph at a flow rate of 1 mL/min. Quantification of CUR was performed at λ = 426 nm, determined using a calibration curve constructed with chromatography-grade CUR (99.2% purity) (AK Scientific, USA): Area =199119.292 (CUR concentration) – 13148.923 (R^2 = 0.999). The detection and quantification limits of CUR were 0.311 and 0.942 mg/L, respectively.

The particle size (φ) and zeta potential (ζ) were determined using a Zetasizer Nano ZS90 analyzer (Malvern Instruments Ltd., Worcester, UK) at 25°C. Particle size was measured without dilution or acidification of the extract, using dynamic light scattering with an M3-PALS analyzer (Kim *et al*., 2019), and an absorption index of 0.05, using a DTS0012 cell. The refractive index was previously determined as 1.340. Zeta potential was measured using electrophoresis and laser Doppler velocimetry, employing a DTS 1060 capillary cell (Morteza-Semnani *et al*., 2022).

Data analysis

Data were analyzed using Statgraphics Centurion XVII software. Analysis of variance (ANOVA) was conducted at a significance level of 5%.

Results

Micellar extraction process

Table 1 presents the experimental design and the mean values of the dependent variables for the micellar extraction process. Additionally, Figure 1 displays the surface and volume response graphs of bioactive compounds.

Total phenolic content

Mean TPC values ranged from 86.1 to 181.0 mg GAE/g turmeric db. ANOVA revealed significant differences ($P < 0.05$) only concerning the turmeric/MS_{SO} ratio. These results are comparable to those reported by Singh *et al*. (2022) for microwave-assisted extraction using 95% ethanol (178.4 ± 4.8 mg GAE/g turmeric db). They are notably higher than those reported by Ivanović *et al*. (2021) for hydrodistillation extraction at 130°C (2.80 ± 0.19 mg GAE/g turmeric), highlighting the influence of both the solvent and the extraction method.

Figure 1A illustrates the TPC response, showing an increase in TPC as the turmeric/MS_{SO} ratio decreases. This trend is attributed to enhanced solvation of bioactive compounds due to the increased presence of MS_{SO}, which provides a greater number of micelles for turmeric. These micelles facilitate the solubilization and subsequent extraction of bioactive compounds (Śliwa and Śliwa, 2020). Similar findings have been reported by Ahmed *et al*. (2023) and Niazmand *et al*. (2021).

Table 1. Results of the experimental design of the micelle extraction process.

Run	Independent variables			Dependent variables					
	Turmeric/ MS	Surfactant (%)	t_E (min)	TPC (mg GAE/g turmeric db)	DPPH• (mg TE/g turmeric db)	$ABTS^{•+}$ (mg TE/g turmeric db)	CUR (mg/g turmeric db)	Particle size (nm)	Zeta potential (mV)
1	0.03	0.7975	10	112.0	37.0	117.9	10.5	211.4	–84.5
2	0.03	0.0700	10	128.8	31.4	64.2	9.6	410.2	–35.5
3	0.03	0.7975	15	129.5	47.6	114.5	3.3	187.4	–77.7
4	0.05	1.5250	5	115.2	32.8	84.3	8.6	216.3	–75.9
5	0.03	0.7975	10	141.5	43.2	120.2	9.4	185.1	–78.6
6	0.03	1.5250	10	155.6	40.8	117.4	10.9	192.8	–79.1
7	0.05	0.7975	10	86.1	27.1	69.0	4.4	207.4	–78.4
8	0.01	0.0700	15	140.3	64.2	120.8	4.0	484.2	–100.3
9	0.01	0.7975	10	181.0	56.3	176.2	7.1	183.7	–82.5
10	0.05	0.0700	15	89.1	23.3	53.9	6.0	371.0	–30.6
11	0.01	1.5250	15	137.5	54.9	143.5	9.4	165.5	–91.3
12	0.05	0.0700	5	99.0	17.1	35.8	8.3	395.7	–33.3
13	0.03	0.7975	10	118.5	52.6	121.2	6.1	198.0	–78.6
14	0.03	0.7975	10	153.8	45.8	110.7	8.2	190.9	–74.4
15	0.01	0.0700	5	178.2	57.8	96.9	5.9	380.5	–95.1
16	0.05	1.5250	15	116.6	48.2	109.2	7.8	219.7	–77.3
17	0.03	0.7975	5	143.8	37.9	100.7	6.7	199.3	–80.1
18	0.03	0.7975	10	130.8	44.9	121.5	6.4	197.9	–77.6
19	0.01	1.5250	5	154.7	68.5	146.6	11.6	172.6	–85.2

ABTS, 2,2′-azino-bis (3-ethylbenzothiazoline-6-sulfonic acid; CUR, curcumin; DPPH, 2,2-Diphenyl-1-picrylhydrazyl; MS, micellar solution; TPC, total phenolic content.

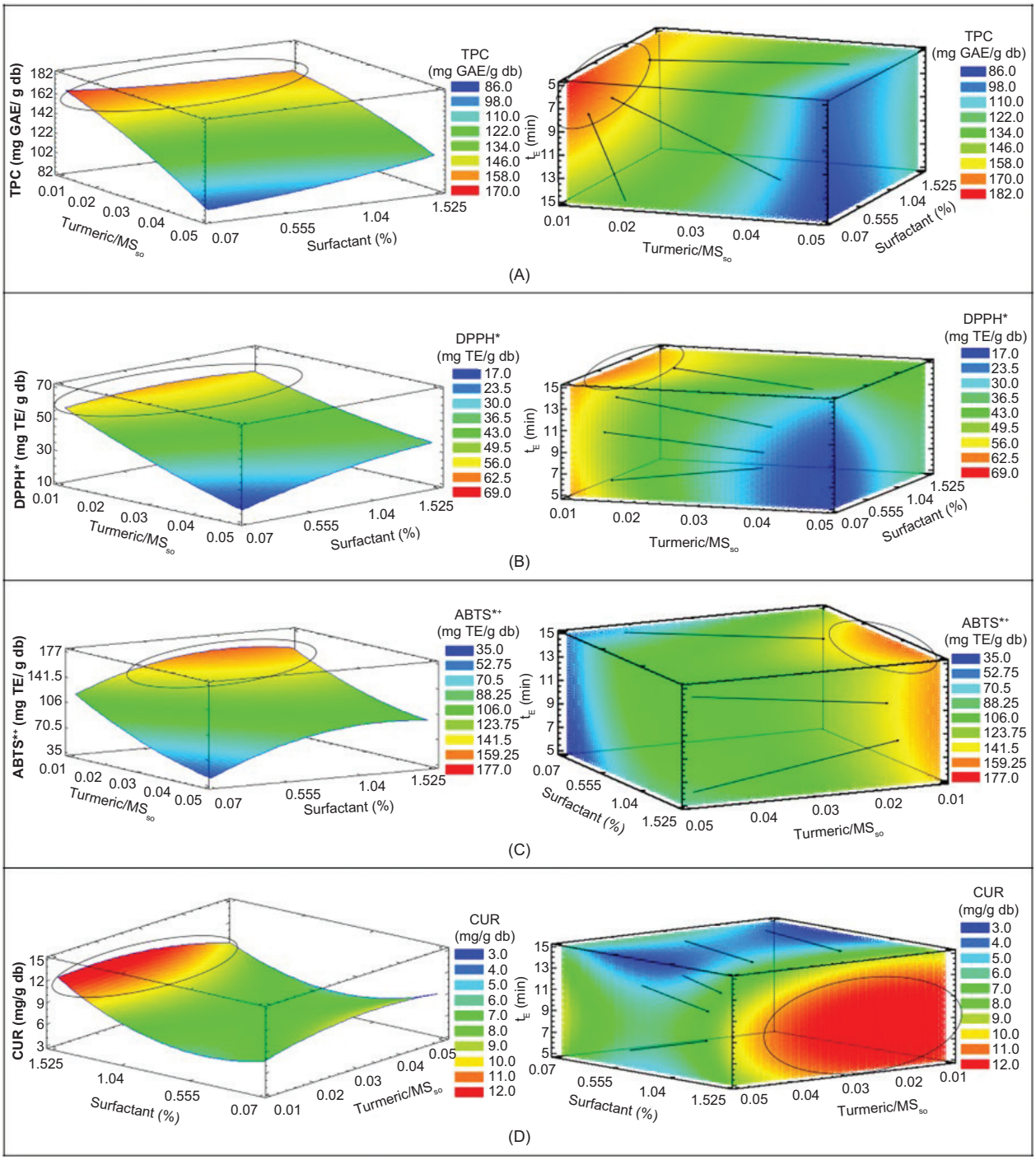

Figure 1. Surface and volume response graphs of TPC (A), DPPH$^{\bullet}$ (B), ABTS$^{\bullet+}$ (C), and CUR (D) bioactive compounds in the micellar extraction.

The optimal conditions for maximizing the TPC (red zone) were: turmeric/MS$_{SO}$ = 0.01–0.02; surfactant = 0.07–1.04%; and t_E = 5–13 min. Skrypnik and Novikova (2020) reported higher TPC extraction at a Tween 80 concentration of 1.14% and an apple/MS ratio of 0.0096 g/mL, which closely aligns with the minimum value in the present study.

Antioxidant capacity

The mean values of DPPH$^{\bullet}$ and ABTS$^{\bullet+}$ ranged between 17.1–68.5 and 35.8–176.2 mg TE/g turmeric db, respectively. These results are notably higher than those reported in the literature. For instance, Papayrata *et al.* (2024) reported a DPPH$^{\bullet}$ value of approximately 19 mg TE/g turmeric db using 80% methanol at 37°C for 12 h.

Wu *et al*. (2024) reported an ABTS$^{\bullet+}$ value of 0.425 mg TE/g dry basis (db) via ethanolic extraction at room temperature for 24 h. Additionally, Ivanović *et al*. (2021) and Şahin (2018) reported ABTS$^{\bullet+}$ values of 40 mg and 29.2 ± 1.1 mg TE/g db, respectively, using ultrasound-assisted ethanol extraction.

These findings suggest that micellar extraction is capable of extracting both lipophilic and hydrophilic bioactive compounds, whereas ethanol primarily targets phenolic bioactive compounds due to the polarity of the solvent (Calle Chumo *et al*., 2022; Rumpf *et al*., 2023). Turmeric is known to be rich in both lipophilic and hydrophilic bioactive compounds (Friesen *et al*., 2019), which explains the higher ABTS$^{\bullet+}$ values observed in comparison to DPPH$^{\bullet}$. Since DPPH$^{\bullet}$ is soluble in organic media, it predominantly reacts with lipophilic bioactive compounds, resulting in lower sensitivity to certain antioxidants (Rumpf *et al*., 2023). In contrast, ABTS$^{\bullet+}$ is more suitable for evaluating antioxidant capacity, especially in samples containing hydrophilic compounds or pigments (Faria *et al*., 2021).

ANOVA revealed significant differences ($P < 0.05$) for both assays (DPPH$^{\bullet}$ and ABTS$^{\bullet+}$) concerning turmeric/MS_{SO} ratio and surfactant. Additionally, DPPH$^{\bullet}$ showed significant variation with the linear interaction between turmeric/MSSO–surfactant, while the quadratic interaction between tE and ABTS$^{\bullet+}$ significantly influenced ABTS$^{\bullet+}$. Figures 1B and 1C display trends for DPPH$^{\bullet}$ and ABTS$^{\bullet+}$ that closely mirror those observed for TPC. The influence of the turmeric/MS_{SO} ratio on antioxidant capacity is evident, as higher surfactant levels enhance the solubilization of bioactive compounds by increasing the availability of sodium oleate (Motikar *et al*., 2021; Śliwa and Śliwa, 2020). Motikar *et al*. (2021) observed a similar effect in the micellar extraction of pomegranate peel/MS (1:30 → 1:100), where DPPH$^{\bullet}$ increased from 78.2 to 84.4%. ABTS$^{\bullet+}$ values increased consistently with increasing surfactant concentration, whereas DPPH$^{\bullet}$ increased only at a high turmeric/MSSO ratio (0.05). Motikar *et al*. (2021) also reported a similar trend for ABTS$^{\bullet+}$ when increasing surfactant concentration (4 → 8% v/v).

For DPPH$^{\bullet}$, the positive interaction between turmeric/MS_{SO} and surfactant is demonstrated by its increase at lower values of both variables. In contrast, the ABTS$^{\bullet+}$ response exhibits a curvilinear trend concerning the surfactant–surfactant interaction, initially increasing and then reaching an asymptote at higher surfactant values (1.525%), indicating a stronger interaction between surfactant and bioactive compounds.

The optimal conditions for maximizing antioxidant capacity (red zone) were as follows:

- DPPH$^{\bullet}$: turmeric/MS_{SO} = 0.01–0.02; surfactant and t_E across the entire range
- ABTS$^{\bullet+}$: turmeric/MS_{SO} = 0.01–0.02; surfactant = 0.555–1.525%; t_E across the full range

Curcumin

The mean CUR values ranged from 3.3 to 11.6 mg/g turmeric dry basis (db). ANOVA revealed significant differences ($P < 0.05$) concerning both surfactant and surfactant–surfactant interactions. To date, there are no reports in the literature on the micellar extraction of CUR using sodium oleate as a surfactant. Park *et al*. (2022) reported CUR values ranging from 8.3–9.4 mg/g turmeric db using 70% ethanol for 2 h at 100°C, attributing the variation to differences in rhizome drying methods. Gilda *et al*. (2010) reported a higher yield of 20.3 mg/g turmeric db using Gelucire 44/14 as surfactant.

Other studies have highlighted the considerable variability in CUR content, which is influenced by the initial bioactive compounds composition in turmeric. This composition is affected by environmental factors such as light exposure, ultraviolet radiation, and temperature (Li *et al*., 2020a). Additionally, extraction efficiency is influenced by several factors, including the polarity, viscosity, and surface tension of the solvent, as well as the extraction temperature and the solute–solvent ratio, among others (Array *et al*., 2018; Patil *et al*., 2019; Sepahpour *et al*., 2018).

Figure 1D presents the response surface graphs for CUR. A curvilinear (convex) increase in CUR is observed with increasing surfactant, attributed to the affinity between micelles and CUR; similar to the trends observed for TPC, DPPH$^{\bullet}$, and ABTS$^{\bullet+}$. Additionally, the surfactant–surfactant interaction reveals a minimum CUR value when the surfactant levels range between 0.070 and 0.555%.

Alibade *et al*. (2020) reported a similar trend in the extraction of antioxidants from residual by-products during cloud point micellar extraction, although they selected lower surfactant levels due to cost considerations. Similarly, Guo *et al*. (2019) observed an increase in polyphenols and alkaloids extracted from mulberry leaves during cloud point micellar extraction using Triton X-114.

The optimal conditions for maximizing CUR (red zone) within the studied region were: turmeric/MS_{SO} = 0.01–0.045, surfactant = 1.525%, and t_E across the entire range.

Elsewhere, Figure 2 presents the surface and volume response graphs of particle size and zeta potential, as well as the pH behavior in the micellar extraction process.

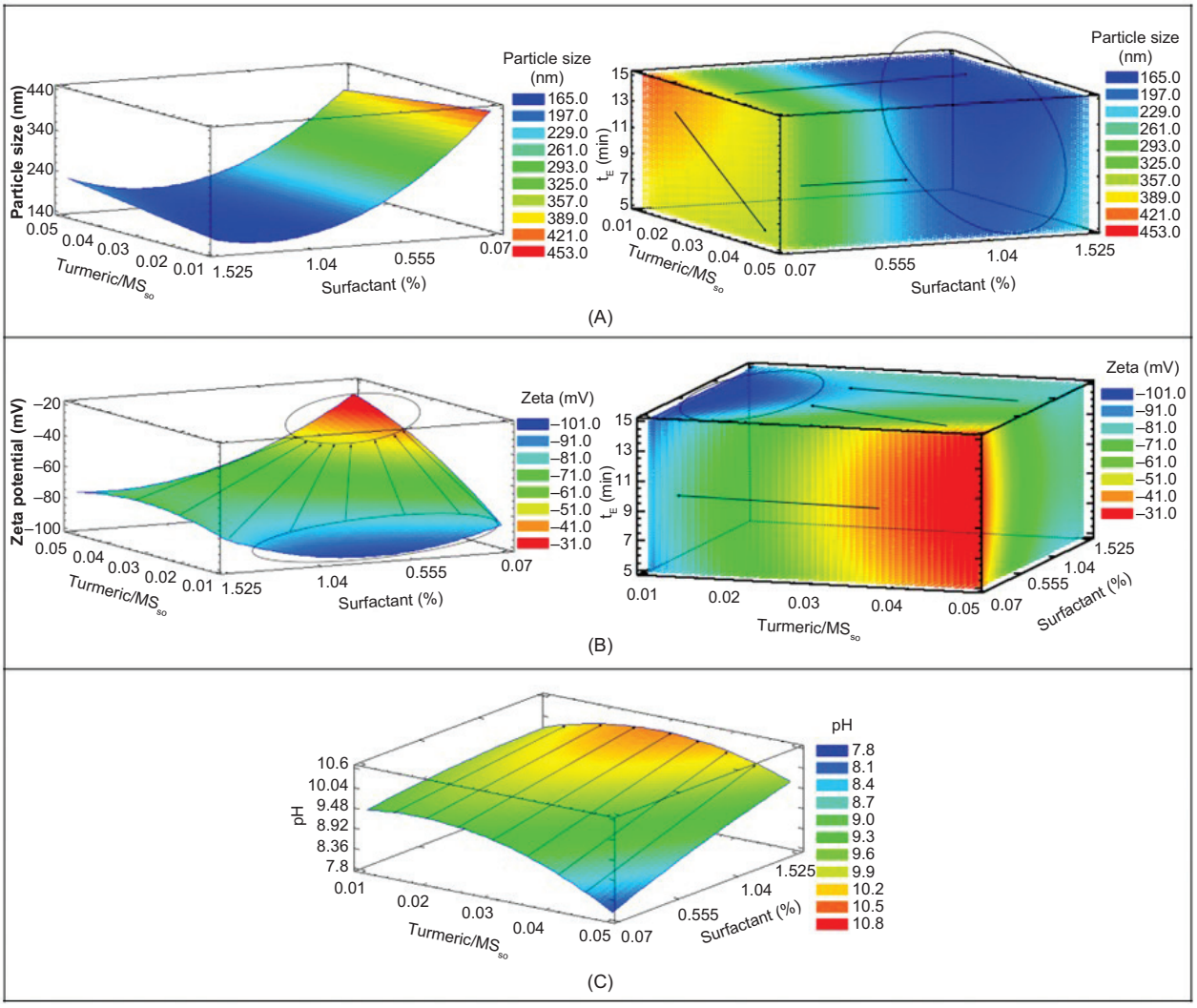

Figure 2. Surface and volume response graphs of particle size (A) and zeta potential (B), and pH behavior (C) in the micellar extraction.

Particle size

The mean particle size values ranged from 165.5 to 484.2 nm. ANOVA revealed significant differences ($P < 0.05$) concerning surfactant, the surfactant–surfactant interaction, and the turmeric/MS$_{SO}$–surfactant linear interaction. Gontsarik *et al.* (2018) and Suga *et al.* (2016) have linked the particle size of MS to pH. In this context, Figure 2C shows an increase in the pH of the extract with increasing surfactant, with the highest values observed when turmeric/MS$_{SO}$ was between 0.03 and 0.05. Suga *et al.* (2016) reported different structural forms in aqueous sodium oleate solutions depending on pH: cubosomes at pH 7.5, vesicles at pH 8.5, and micelles ($\varphi < 50$ nm) and vesicles ($\varphi < 1000$ nm) at pH 9.7–10.1. Additionally, Gontsarik *et al.* (2018) reported particle size values ranging from 200 to 300 nm in cubosomes formed from oleic acid self-assembled systems with human cathelicidin LL-37 in aqueous solution.

Figure 2A presents the particle size response graphs during the micellar extraction of turmeric, where a decrease in particle size is observed with increasing surfactant. This trend is consistent with previous findings and is attributed to the enhanced formation of micellar structures of sodium oleate (Ogino *et al.*, 1988), particularly when concentrations exceed the CMC of 0.033% w/w (Sergeev *et al.*, 2022). Additionally, the largest particle size values occur when the extract exhibits a low pH.

Smaller particle size values suggest a greater number of micelles, which enhances the extraction of bioactive compounds due to an increased interaction with surfactant and improved extract stability (Li *et al.*, 2020b; Wu *et al.*, 2016). Furthermore, the turmeric/MS–surfactant interaction was positive, indicating that particle size increases when both turmeric/MS$_{SO}$ and surfactant decrease. This condition corresponds to a high electrical

potential (ζ ≈ −80 and −90 mV), which may contribute to the expansion of micellar structures. Finally, the conditions of the independent variables that minimize zeta potential are illustrated in the blue zone, where surfactant = 0.555–0.525%, and turmeric/MS_{SO} and t_E span the entire range.

Zeta potential

The mean zeta potential values ranged from −100.3 to −30.6 mV, indicating a strong negative electrical potential that supports the physicochemical stability of the system due to the predominance of repulsive forces (|ζ| > 30 mV) (Pinheiro *et al*., 2020; Sun *et al*., 2016). ANOVA revealed significant differences (P < 0.05) concerning turmeric/MS_{SO} and surfactant, as well as the turmeric/MS_{SO}–surfactant and surfactant–surfactant interactions. The high negative electrical potential is primarily attributed to the increase in surfactant (Bhattarai *et al*., 2018) and the alkaline pH of the extracts (7.8–10.1) (Cacua *et al*., 2019). Figure 2B presents the zeta potential response graphs during the micellar extraction of turmeric, showing an increase in electric potential with increasing surfactant, particularly when turmeric/MS_{SO} is formulated at 0.01. This behavior is attributed to the anionic nature of sodium oleate, which enhances the negative electric potential in the surface layer (Bhattarai *et al*., 2018).

The presence of co-ions in the MS also influences micellar structure and zeta potential (Santos *et al*., 2017), suggesting that ions contributed by turmeric play a significant role in this phenomenon. A lower negative electric potential is observed at low surfactant levels (0.07–0.555%), along with increasing turmeric/MS_{SO} (red zone), likely due to the higher content of bioactive compounds and their interaction with the MS. Śliwa and Śliwa (2020) and Śliwa *et al*. (2019) described this condition as a neutralizing effect on zeta potential, where lower surfactant (fewer micelles) is more susceptible to the incorporation of bioactive compounds, thereby reducing the surface charge.

The t_E was not a critical factor in the micellar extraction of turmeric in the findings reported by Zhang *et al*. (2016) in microwave-assisted micellar extraction of *Sophora flavescens* Ait alkaloids, and by Mandal and Lahiri (2022) in cloud point micellar extraction of beryllium and chromium. However, other studies have identified t_E as an influential variable (Motikar *et al*., 2021; Skrypnik and Novikova, 2020). Finally, the conditions that favored a higher negative electric potential (blue zone) were: turmeric/MS_{SO} = 0.01–0.03; t_E = 15 min; and surfactant across the entire range.

Mathematical modelling and experimental optimization of multiple responses

Table 2 presents the regression and determination coefficients (R^2) for the models of the dependent variables. Most of the R^2 values account for over 80% of the variability in the experimental data, indicating a good model fit. However, the model for CUR showed the lowest acceptable R^2 value (76.0%), likely due to its sensitivity to processing conditions or other factors that introduce high variability, thereby limiting its predictive accuracy.

Additionally, ANOVA results indicated that most models exhibited statistically significant effects (P < 0.05), except

Table 2. Regression and determination (R^2) coefficients of the mathematical models of the dependent variables.

Coefficient	TPC	DPPH•	ABTS•+	CUR	ϕ	ζ
Intercept	210.6	86.4	108.1	0.25	391.2	–123.7
Turmeric/MS	–1662.8	–1759.8	–3606.3	230.4	217.2	2439.8
Surfactant	–32.3	10.0	97.0	–5.8	–489.8	–34.4
t_E	–2.2	–3.1	5.6	1.3	9.5	3.9
Turmeric/MS – Turmeric/MS	–13810.6	6094.0	24219.1	–3220.7	530.5	–17701.2
Turmeric/MS – Surfactant	601.8	337.5	270.3	–78.7	1683.0	–929.7
Turmeric/MS – t_E	58.3	35.9	27.8	1.1	–147.4	15.9
Surfactant – Surfactant	5.9	–5.9	–41.8	6.1	200.7	30.3
Surfactant – t_E	1.1	–0.4	–0.7	0.04	–2.9	–0.2
t_E – t_E	–0.1	0.1	–0.2	–0.08	–0.1	–0.2
R^2	80.6	90.1	93.3	76.0	98.1	87.0
Adjust (P)	0.0226*	0.0015*	0.0003*	0.0503	0.0000*	0.0046*

*Significance (P < 0.05).
ABTS, 2,2′-azino-bis (3-ethylbenzothiazoline-6-sulfonic acid; CUR, curcumin; DPPH, 2,2-Diphenyl-1-picrylhydrazyl; MS, micellar solution; TPC, total phenolic content.

the CUR ($P > 0.05$), suggesting that the behavior of CUR is only partially explained by the model. This limitation may be attributed to the potential degradation of CUR under alkaline conditions (Cano-Higuita *et al*., 2015).

Table 3 presents the criteria, impacts, and sensitivity parameters established for the experimental optimization of the micellar extraction of bioactive compounds from turmeric. The overall desirability reached 70.9%, with the optimal conditions for the independent variables defined as follows: turmeric/MS_{SO} = 0.01 g/g; surfactant = 1.525%; and t_E = 6.64 min. Additionally, the validation of the mathematical models yielded MRE values of up to 16.2%, which is considered acceptable according to Castaño-Peláez *et al*. (2022). These results demonstrate a good degree of fit for the models, consistent with the desirability function used for multiresponse optimization. Moreover, they validate the predictive ability of the developed models, confirming the effectiveness of the statistical approach applied for their optimization.

Comparison of extraction methodologies

Figure 1 presents a comparison of the TPC, DPPH•, $ABTS^{•+}$, and CUR results from conventional extraction and micellar extraction, along with the corresponding P-values from the t-test. The results show that the mean values of TPC, DPPH•, and $ABTS^{•+}$ were significantly higher in the micellar extraction compared to conventional extraction ($P < 0.05$), whereas the CUR content was significantly lower ($P < 0.05$).

The higher TPC, DPPH•, and $ABTS^{•+}$ values observed in the micellar extract are attributed to the ability of micelles to interact with a broad range of bioactive compounds, both lipophilic and hydrophilic, when amphiphilic molecules are employed during their extraction (Ziyatdinova and Budnikov, 2021). The TPC results suggest that micellar extraction has a greater capacity to extract phenolic bioactive compounds beyond CUR, including demethoxycurcumin, bisdemethoxycurcumin, cyclocurcumin, β-sesquiphellandrene, α-curcumene, ar-turmerone, and α/β-turmerone, among others (Tyagi *et al*., 2015). Ziyatdinova *et al*. (2016) reported comparable values in ultrasound-assisted micellar extraction (surfactant: Brij 35) for phenolic antioxidants extracted from cinnamon, which showed an improvement of over 100% compared to conventional extraction methods. These findings were further validated in extracts from cloves, oregano, and black pepper. Similarly, compared to traditional extraction techniques, He *et al*. (2015) achieved a yield improvement of over 90% in the purification of lecithin from black beans using micellar extraction based on sodium bis(2-ethylhexyl) sulfosuccinate.

However, the Folin–Ciocalteu method is known to be affected by interferences from reducing sugars, which can lead to an overestimation of TPC (Briones Muñoz and Riera, 2020). In this context, the micellar extraction may promote a certain degree of alkaline hydrolysis of the starch present, resulting in the formation of reducing sugars due to the elevated pH and increased extraction temperature (Lawag *et al*., 2023). Furthermore, the difference between $ABTS^{•+}$ and DPPH• values is more pronounced in the micellar extraction than in the conventional extracts. This difference is likely due to the broader range of bioactive compounds extracted by the micellar extraction compared to ethanol-based extraction, which is limited by its polarity (Calle Chumo *et al*., 2022; Ziyatdinova and Budnikov, 2021).

The higher extraction of CUR with ethanol is attributed to the strong chemical affinity between them, as reported by various authors (Fernández-Marín *et al*., 2021; Rezaei *et al*., 2023; Yang *et al*., 2020). Additionally, it has been demonstrated that the degradation of CUR is pH-dependent, occurring more slowly under acidic conditions (pH < 7) and accelerating in alkaline environments, particularly at pH values near 10.8. Additionally, elevated temperatures

Table 3. Multiresponse optimization parameters for the micelle extraction.

Independent variables	Criteria	Impact	Sensibility	Model value	Experimental value	MRE (%)
TPC (mg GAE/g turmeric db)	Maximize	5.0	Alto	161.9	181.6 ± 3.0	12.1
DPPH• (mg TE/g turmeric db)	Maximize	5.0	Alto	60.4	50.6 ± 1.1	16.2
$ABTS^{•+}$ (mg TE/g turmeric db)	Maximize	5.0	Alto	151.6	142.7 ± 7.9	5.8
CUR (mg/g turmeric db)	Maximize	5.0	Alto	12.2	11.6	5.2
φ (nm)	Minimize	4.0	Medio	160.1	178.6 ± 7.7	11.6
ζ (mV)	Minimize	4.0	Medio	–81.6	–80.6 ± 4.6	1.3

ABTS, 2,2′-azino-bis (3-ethylbenzothiazoline-6-sulfonic acid; CUR, curcumin; DPPH, 2,2-Diphenyl-1-picrylhydrazyl; MRE, mean relative error; TPC, total phenolic content.

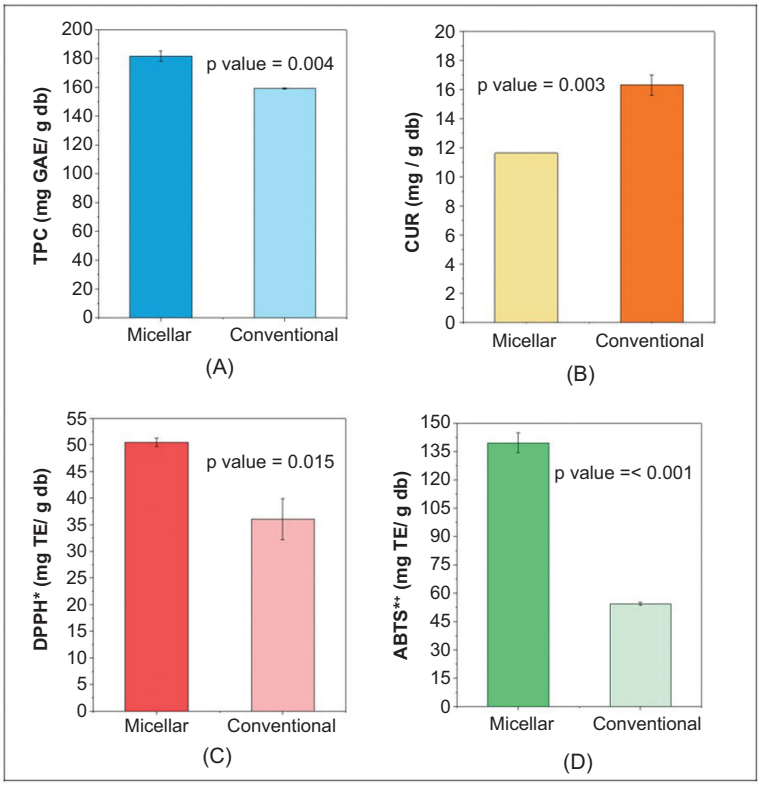

Figure 3. Comparison of TPC (A), CUR (B), DPPH• (C), and ABTS•+ (D), based on extraction technologies and P-values of t-test

Table 4. Energy requirements and costs of micellar and conventional curcumin (CUR) extraction.

Extraction	t_E (min)	Ratio turmeric/MS	Yield (mg CUR/g turmeric db)	Energy consumption (GJ/g CUR)	Cost ($US/g CUR)
Conventional	60.0	0.04	16.3 ± 0.7	12.0	555.0
Micellar	6.4	0.01	11.6	3.8	83.3

Temperature: 35°C (Conventional) y ambient (Micellar extraction).
CUR, curcumin; MS, micellar solution.

further promote its decomposition (Aboudiab *et al.*, 2020). These findings suggest that the extraction conditions used in this study (alkaline pH and the temperature increase associated with high-speed homogenization) could have contributed to an accelerated degradation rate of CUR. However, the health benefits of CUR have been shown to increase when it acts synergistically with other bioactive compounds present in turmeric (Panda *et al.*, 2021). In general, the results were influenced by several factors, including kinetic parameters, radical sensitivity, adduct formation, reaction mechanisms, and the characteristics of the extract, among others (Ilyasov *et al.*, 2020; Rumpf *et al.*, 2023).

Table 4 presents the energy requirements and costs associated with micellar and conventional CUR extraction. The data indicate that micellar extraction results in lower energy consumption (by 68.3%), yield (by 28.8%), and production costs (by 85.0%) compared to the conventional extraction methods. Importantly, micellar extraction is easier to scale up, and the necessary equipment is readily available. In contrast, conventional extraction relies on heating in water bath, which poses limitations in terms of space and production capacity.

Several studies have evaluated the extraction of bioactive compounds using green technologies, showing a wide range of extraction yields. For instance,

microwave-assisted extraction using acetone achieved a yield of 53.9% (Sahne *et al*., 2016), while subcritical water extraction modified with ethanol reached up to 152% (Rezaei *et al*., 2023), although this method requires high temperatures (90°C) and increased pressure (2 MPa). Similarly, supercritical CO_2 extraction has shown yields around 102.4%; however, it requires elevated pressures (25 MPa) and prolonged extraction times (90 min), leading to high energy consumption (Chhouk *et al*., 2017).

In comparison, the micellar extraction developed in this study achieved a yield of 75.2%, comparable to that obtained with ionic liquids: 74.3% without ultrasound and 86.7% with ultrasound assistance (Patil *et al*., 2021). In addition to the favorable yield, micellar extraction presents several advantages over other nonconventional techniques: (1) it can be easily scaled up using conventional equipment, (2) it requires very short extraction times (below 7 min), and (3) it operates under mild conditions without the need for high pressure or temperature. These benefits, combined with its low energy consumption and the use of food-grade, safe compounds, highlight micellar extraction as a promising and sustainable green technology for the recovery of bioactive compounds.

Conclusion

In general, the micellar extraction of turmeric is primarily influenced by the turmeric/MS_{SO} and the surfactant, with optimal performance observed at higher levels of both micellar sodium oleate and surfactant. These conditions enhance the interaction between MS_{SO} and the bioactive compounds of turmeric. Additionally, higher surfactant concentrations increase the number of micelles available to interact with turmeric, thereby improving solubilization of bioactive compounds and the overall efficiency of the micellar extraction process. Contrary to the expectations, t_E was not a critical factor, suggesting that the solubilization of bioactive compounds occurs rapidly.

Micellar extraction demonstrated higher TPC and antioxidant capacity compared to conventional extraction, while also requiring less energy and incurring lower associated costs. In this context, micellar extraction emerges as a cost-effective and environmentally friendly technology that delivers acceptable yields. It is therefore considered a promising alternative for industrial-scale applications.

Acknowledgments

The authors gratefully acknowledge the financial support of the National University of Colombia, Medellín, Antioquia, and Inbiotech S.A.S., Manizales, Caldas, Colombia.

Author Contributions

All authors contributed equally to this article.

Conflicts of Interest

None.

Funding

This research project was financially supported by Inbiotech S.A.S. (56838), Manizales, Caldas, Colombia.

References

Aboudiab, B., Tehrani-Bagha, A.R. and Patra, D., 2020. Curcumin degradation kinetics in micellar solutions: Enhanced stability in the presence of cationic surfactants. Colloids and Surfaces A: Physicochemical and Engineering Aspects. 592: 124602. https://doi.org/10.1016/j.colsurfa.2020.124602

Ahmed, T., Rana, M.R., Hossain, M.A., Ullah, S. and Suzauddula, M., 2023. Optimization of ultrasound-assisted extraction using response surface methodology for total anthocyanin content, total phenolic content, and antioxidant activities of Roselle (*Hibiscus sabdariffa* L.) calyces and comparison with conventional Soxhlet extraction. Biomass Conversion and Biorefinery. 14: 28985–28999. https://doi.org/10.1007/s13399-023-03881-y

Alibade, A., Batra, G., Bozinou, E., Salakidou, C. and Lalas, S., 2020. Optimization of the extraction of antioxidants from winery wastes using cloud point extraction and a surfactant of natural origin (lecithin). Chemical Papers. 74(12): 4517–4524. https://doi.org/10.1007/s11696-020-01269-0

Array, E.J., Tonfack Djikeng, F., Kingne Kingne, F., Kingne, E.E. and Womeni, H.M., 2018. Effect of different extraction solvents on the phenolic content and antioxidant activity of turmeric (*Curcuma longa*) from South-West Region, Cameroon. Food Research. 3(1): 86–90. https://doi.org/10.26656/fr.2017.3(1).227

Azooz, E.A., Ridha, R.K. and Abdulridha, H.A., 2021. The fundamentals and recent applications of micellar system extraction for nanoparticles and bioactive molecules: A review. Nano Biomedicine and Engineering. 13(3): 264–278. https://doi.org/10.5101/nbe.v13i3.p264-278

Bhattarai, A., Chatterjee, S. and Niraula, T.P., 2018. Studies on the behavior of anionic surfactant sodiumdodecyl sulphate (SDS). LAP LAMBERT Academic Publishing. Available from: https://www.researchgate.net/publication/327105815_Studies_on_the_Behavior_of_Anionic_Surfactant_Sodiumdodecyl_Sulphate_SDS

Briones Muñoz, S. and Riera, M.A., 2020. Residuos de la cáscara de yuca y cera de abejas como potenciales materiales de partida para la producción de bioplásticos. Avances En Química. 15(1): 3–11. https://doi.org/10.53766/AVANQUIM/2020.15.01.01

Cacua, K., Ordoñez, F., Zapata, C., Herrera, B., Pabón, E. and Buitrago-Sierra, R., 2019. Surfactant concentration and pH effects on the zeta potential values of alumina nanofluids to inspect stability. Colloids and Surfaces A: Physicochemical and Engineering Aspects. 583: 123960. https://doi.org/10.1016/j.colsurfa.2019.123960

Calle Chumo, R.N., Calle Chumo, D.A., Gallegos Peredo, A.S. and Jarrin Oseguera, P.I., 2022. Influence of the solvent on the extraction of phenolic compounds from the coffee grounds by Soxhlet leaching. Ingeniería e Investigación. 43(1): e97521. https://doi.org/10.15446/ing.investig.97521

Cano-Higuita, D.M., Vélez, H.A.V. and Telis, V.R.N., 2015. Microencapsulation of turmeric oleoresin in binary and ternary blends of gum arabic, maltodextrin and modified starch. Ciência e Agrotecnologia. 39(2): 173–182. https://doi.org/10.1590/S1413-70542015000200009

Castaño-Peláez, H.I., Cortés-Rodríguez, M., Gil-González, J. and Gallón-Bedoya, M., 2022. Influence of gum arabic and homogenization process on the physicochemical stability of strawberry suspensions. Food Science and Technology. 42: 58020. https://doi.org/10.1590/fst.58020

Chhouk, K., Wahyudiono, W., Kanda, H. and Goto, M., 2017. Comparison of conventional and ultrasound assisted supercritical carbon dioxide extraction of curcumin from turmeric (*Curcuma longa* L.). Engineering Journal. 21(5): 53–65. https://doi.org/10.4186/ej.2017.21.5.53

Doldolova, K., Bener, M., Lalikoğlu, M., Aşçı, Y.S., Arat, R. and Apak, R., 2021. Optimization and modeling of microwave-assisted extraction of curcumin and antioxidant compounds from turmeric by using natural deep eutectic solvents. Food Chemistry. 353: 129337. https://doi.org/10.1016/j.foodchem.2021.129337

Dong, D., Quan, E., Yuan, X., Xie, Q., Li, Z. and Wu, B., 2017. Sodium oleate-based nanoemulsion enhances oral absorption of chrysin through inhibition of UGT-mediated metabolism. Molecular Pharmaceutics. 14(9): 2864–2874. https://doi.org/10.1021/acs.molpharmaceut.6b00851

Esparza, I.-N., 2021. Cúrcuma (Curcuma longa): Una revisión bibliográfica del procesamiento, propiedades funcionales y capacidad antimicrobiana. 120. Available from: https://repositorio.uchile.cl/bitstream/handle/2250/181556/Curcuma-curcuma-longa-una-revision-bibliografica-del-procesamiento.pdf?sequence=1

Faria, J.V., Valido, I.H., Paz, W.H.P., da Silva, F.M.A., de Souza, A.D.L., Acho, L.R.D., *et al*. 2021. Comparative evaluation of chemical composition and biological activities of tropical fruits consumed in Manaus, central Amazonia, Brazil. Food Research International. 139: 109836. https://doi.org/10.1016/j.foodres.2020.109836

Fernández-Marín, R., Fernandes, S.C.M., Andrés, M.A. and Labidi, J., 2021. Microwave-assisted extraction of *Curcuma longa* L. oil: Optimization, chemical structure and composition, antioxidant activity and comparison with conventional Soxhlet extraction. Molecules. 26(6): 1516. https://doi.org/10.3390/molecules26061516

Friesen, J.B., Liu, Y., Chen, S.-N., McAlpine, J.B. and Pauli, G.F., 2019. Selective depletion and enrichment of constituents in "Curcumin" and other *Curcuma longa* preparations. Journal of Natural Products. 82(3): 621–630. https://doi.org/10.1021/acs.jnatprod.9b00020

Fuloria, S., Mehta, J., Chandel, A., Sekar, M., Rani, N.N.I.M., Begum, M.Y., *et al*. 2022. A comprehensive review on the therapeutic potential of *Curcuma longa* Linn. in relation to its major active constituent curcumin. Frontiers in Pharmacology, 13: 820806. https://doi.org/10.3389/fphar.2022.820806

Gilda, S., Kanitkar, M., Bhonde, R. and Paradkar, A., 2010. Activity of water-soluble turmeric extract using hydrophilic excipients. LWT – Food Science and Technology. 43(1): 59–66. https://doi.org/10.1016/j.lwt.2009.07.004

Gökdemir, B., Baylan, N. and Çehreli, S., 2020. Application of a novel ionic liquid as an alternative green solvent for the extraction of curcumin from turmeric with response surface methodology: Determination and optimization study. Analytical Letters. 53(13): 2111–2121. https://doi.org/10.1080/00032719.2020.1730394

Gontsarik, M., Mohammadtaheri, M., Yaghmur, A. and Salentinig, S., 2018. pH-Triggered nanostructural transformations in antimicrobial peptide/oleic acid self-assemblies. Biomaterials Science. 6(4): 803–812. https://doi.org/10.1039/C7BM00929A

Guo, N., Jiang, Y.-W., Kou, P., Liu, Z.-M., Efferth, T., Li, Y.-Y., et al. 2019. Application of integrative cloud point extraction and concentration for the analysis of polyphenols and alkaloids in mulberry leaves. Journal of Pharmaceutical and Biomedical Analysis. 167: 132–139. https://doi.org/10.1016/j.jpba.2019.02.002

He, S., Shi, J., Walid, E., Zhang, H., Ma, Y. and Xue, S.J., 2015. Reverse micellar extraction of lectin from black turtle bean (*Phaseolus vulgaris*): Optimisation of extraction conditions by response surface methodology. Food Chemistry. 166: 93–100. https://doi.org/10.1016/j.foodchem.2014.05.156

He, S., Xu, B. and Zhang, Y., 2019. Krafft temperature, critical micelle concentration, and rheology of "Pseudo-Gemini" surfactant comprising fatty acid soap and bola-type quaternary ammonium salt. Journal of Surfactants and Detergents. 22(6): 1269–1277. https://doi.org/10.1002/jsde.12300

Hemlata, Meena, P.R., Singh, A.P. and Tejavath, K.K., 2020. Biosynthesis of silver nanoparticles using *Cucumis prophetarum* aqueous leaf extract and their antibacterial and antiproliferative activity against cancer cell lines. ACS Omega. 5(10): 5520–5528. https://doi.org/10.1021/acsomega.0c00155

Ilyasov, I.R., Beloborodov, V.L., Selivanova, I.A. and Terekhov, R.P., 2020. ABTS/PP decolorization assay of antioxidant capacity reaction pathways. International Journal of Molecular Sciences. 21(3): 1131. https://doi.org/10.3390/ijms21031131

Ivanović, M., Makoter, K. and Islamčević Razboršek, M., 2021. Comparative study of chemical composition and antioxidant activity of essential oils and crude extracts of four characteristic Zingiberaceae herbs. Plants. 10(3): 501. https://doi.org/10.3390/plants10030501

Khani, R., Sheykhi, R. and Bagherzade, G., 2019. An environmentally friendly method based on micro-cloud point extraction for determination of trace amount of quercetin in food and fruit juice samples. Food Chemistry. 293: 220–225. https://doi.org/10.1016/j.foodchem.2019.04.099

Kim, A.R., An, H.J., Jang, E.S., Lee, J.D. and Park, S.N., 2019. Preparation, physical characterization, and in vitro skin permeation of deformable liposomes loaded with taxifolin and taxifolin tetraoctanoate. European Journal of Lipid Science and Technology, 121(6): 201800501. https://doi.org/10.1002/ejlt.201800501

Lawag, I.L., Nolden, E.S., Schaper, A.A.M., Lim, L.Y. and Locher, C., 2023. A modified Folin–Ciocalteu assay for the determination of total phenolics content in honey. Applied Sciences. 13(4): 2135. https://doi.org/10.3390/app13042135

Le-Tan, H. and Jaeger, H., 2022. Impact of cell disintegration techniques on curcumin recovery. Food Engineering Reviews. 14(4): 655–672. https://doi.org/10.1007/s12393-022-09319-x

Li, K., Fu, L., Zhao, Y.-Y., Xue, S.-W., Wang, P., Xu, X.-L., *et al.* 2020a. Use of high-intensity ultrasound to improve emulsifying properties of chicken myofibrillar protein and enhance the rheological properties and stability of the emulsion. Food Hydrocolloids. 98: 105275. https://doi.org/10.1016/j.foodhyd.2019.105275

Li, Y., Kong, D., Fu, Y., Sussman, M.R. and Wu, H., 2020b. The effect of developmental and environmental factors on secondary metabolites in medicinal plants. Plant Physiology and Biochemistry. 148: 80–89. https://doi.org/10.1016/j.plaphy.2020.01.006

Mandal, S. and Lahiri, S., 2022. A review on extraction, preconcentration and speciation of metal ions by sustainable cloud point extraction. Microchemical Journal. 175: 107150. https://doi.org/10.1016/j.microc.2021.107150

Morteza-Semnani, K., Saeedi, M., Akbari, J., Eghbali, M., Babaei, A., Hashemi, S.M.H., *et al.* 2022. Development of a novel nanoemulgel formulation containing cumin essential oil as skin permeation enhancer. Drug Delivery and Translational Research. 12(6): 1455–1465. https://doi.org/10.1007/s13346-021-01025-1

Motikar, P.D., More, P.R. and Arya, S.S., 2021. A novel, green environment-friendly cloud point extraction of polyphenols from pomegranate peels: A comparative assessment with ultrasound and microwave-assisted extraction. Separation Science and Technology. 56(6): 1014–1025. https://doi.org/10.1080/01496395.2020.1746969

Niazmand, R., Shahidi Noghabi, M. and Niazmand, A., 2021. Optimization of subcritical water extraction of phenolic compounds from *Ziziphus jujuba* using response surface methodology: Evaluation of thermal stability and antioxidant activity. Chemical and Biological Technologies in Agriculture. 8(1): 6. https://doi.org/10.1186/s40538-020-00203-6

Ogino, K., Kubota, T., Uchiyama, H. and Abe, M., 1988. Micelle formation and micellar size by a light scattering technique. Available from: https://www.jstage.jst.go.jp/article/jos1956/37/8/37_8_588/_pdf

Othman, R., Abdurasid, M.A., Mahmad, N. and Ahmad Fadzillah, N., 2019. Alkaline-based curcumin extraction from selected Zingiberaceae for antimicrobial and antioxidant activities. Pigment & Resin Technology. 48(4): 293–300. https://doi.org/10.1108/PRT-08-2018-0071

Panda, S.K., Nirvanashetty, S., Missamma, M. and Jackson-Michel, S., 2021. The enhanced bioavailability of free curcumin and bioactive-metabolite tetrahydrocurcumin from a dispersible, oleoresin-based turmeric formulation. Medicine. 100(27): e26601. https://doi.org/10.1097/MD.0000000000026601

Pandey, P., Grover, K., Dhillon, T.S., Kaur, A. and Javed, M., 2021. Evaluation of polyphenols enriched dairy products developed by incorporating black carrot (*Daucus carota* L.) concentrate. Heliyon. 7(5): e06880. https://doi.org/10.1016/j.heliyon.2021.e06880

Papayrata, C., Chumroenphat, T., Saensouk, P. and Saensouk, S., 2024. Diversity of curcuminoids, bioactive compounds and antioxidant activities in three species of Curcuma. Tropical Journal of Pharmaceutical Research. 23(8): 1291–1298. https://doi.org/10.4314/tjpr.v23i8.8

Park, J., Do, S., Lee, M., Ha, S. and Lee, K.-G., 2022. Preparation of turmeric powder with various extraction and drying methods. Chemical and Biological Technologies in Agriculture. 9(1): 39. https://doi.org/10.1186/s40538-022-00307-1

Patil, S.S., Bhasarkar, S. and Rathod, V.K., 2019. Extraction of curcuminoids from *Curcuma longa*: Comparative study between batch extraction and novel three phase partitioning. Preparative Biochemistry and Biotechnology. 49(4): 407–418. https://doi.org/10.1080/10826068.2019.1575859

Patil, S.S., Pathak, A. and Rathod, V.K., 2021. Optimization and kinetic study of ultrasound assisted deep eutectic solvent based extraction: A greener route for extraction of curcuminoids from Curcuma longa. Ultrasonics Sonochemistry. 70: 105267. https://doi.org/10.1016/j.ultsonch.2020.105267

Patil, S.S. and Rathod, V.K., 2020. Synergistic effect of ultrasound and three phase partitioning for the extraction of curcuminoids from *Curcuma longa* and its bioactivity profile. Process Biochemistry. 93: 85–93. https://doi.org/10.1016/j.procbio.2020.02.031

Pinheiro, R.G.R., Granja, A., Loureiro, J.A., Pereira, M.C., Pinheiro, M., Neves, A.R., *et al.* 2020. Quercetin lipid nanoparticles functionalized with transferrin for Alzheimer's disease. European Journal of Pharmaceutical Sciences. 148: 105314. https://doi.org/10.1016/j.ejps.2020.105314

Rangel-Yagui, C.O., Pessoa, A. and Tavares, L.C., 2005. Micellar solubilization of drugs. Journal of Pharmacy & Pharmaceutical Sciences: A Publication of the Canadian Society for Pharmaceutical Sciences, Societe Canadienne Des Sciences Pharmaceutiques. 8(2): 147–165. http://www.ncbi.nlm.nih.gov/pubmed/16124926

Rezaei, F., Eikani, M.H., Nosratinia, F. and Bidaroni, H.H., 2023. Optimization of ethanol-modified subcritical water extraction of curcuminoids from turmeric (*Curcuma longa* L.) rhizomes: Comparison with conventional techniques. Food Chemistry. 410: 135331. https://doi.org/10.1016/j.foodchem.2022.135331

Rumpf, J., Burger, R. and Schulze, M., 2023. Statistical evaluation of DPPH, ABTS, FRAP, and Folin-Ciocalteu assays to assess the antioxidant capacity of lignins. International Journal of Biological Macromolecules. 233: 123470. https://doi.org/10.1016/j.ijbiomac.2023.123470

Şahin, S., 2018. Optimization of ultrasonic-assisted extraction parameters for antioxidants from *Curcuma longa* L. Trakya University Journal of Natural Sciences. 19(2): 121–128. https://doi.org/10.23902/trkjnat.344985

Sahne, F., Mohammadi, M., Najafpour, G. and Moghadamnia, A.A., 2016. Extraction of bioactive compound curcumin from turmeric (*Curcuma longa* L.) via different routes: A comparative study. Pakistan Journal of Biotechnology. 13(3): 173–180.

Santos, M.S., Biscaia, E.C. and Tavares, F.W., 2017. Effect of electrostatic correlations on micelle formation. Colloids and Surfaces A: Physicochemical and Engineering Aspects. 533: 169–178. https://doi.org/10.1016/j.colsurfa.2017.07.079

Sepahpour, S., Selamat, J., Abdul Manap, M., Khatib, A. and Abdull Razis, A., 2018. Comparative analysis of chemical composition, antioxidant activity and quantitative characterization of some phenolic compounds in selected herbs and spices in different solvent extraction systems. Molecules. 23(2): 402. https://doi.org/10.3390/molecules23020402

Sergeev, V.V., Cheremisina, O.V., Fedorov, A.T., Gorbacheva, A.A. and Balandinsky, D.A., 2022. Interaction features of sodium oleate and oxyethylated phosphoric acid esters with the apatite surface. ACS Omega. 7(3): 3016–3023. https://doi.org/10.1021/acsomega.1c06047

Sharma, A., Ray, A. and Singhal, R.S., 2023. Co-extraction of turmeric (*Curcuma longa* L.) and dried coconut shreds by supercritical fluid extraction (SFE): Chemical and bioactivity profile. Journal of Cleaner Production. 382: 135313. https://doi.org/10.1016/j.jclepro.2022.135313

Singh, K., Srichairatanakool, S., Chewonarin, T., Prommaban, A., Samakradhamrongthai, R.S., Brennan, M.A., *et al*. 2022. Impact of green extraction on curcuminoid content, antioxidant activities and anti-cancer efficiency (in vitro) from turmeric rhizomes (*Curcuma longa* L.). Foods. 11(22): 3633. https://doi.org/10.3390/foods11223633

Skrypnik, L. and Novikova, A., 2020. Response surface modeling and optimization of polyphenols extraction from apple pomace based on nonionic emulsifiers. Agronomy. 10(1): 92. https://doi.org/10.3390/agronomy10010092

Śliwa, K. and Śliwa, P., 2020. The accumulated effect of the number of ethylene oxide units and/or carbon chain length in surfactants structure on the nano-micellar extraction of flavonoids. Journal of Functional Biomaterials. 11(3): 57. https://doi.org/10.3390/jfb11030057

Śliwa, P. and Śliwa, K., 2021. Nanomicellar extraction of polyphenols—Methodology and applications review. International Journal of Molecular Sciences. 22(21): 11392. https://doi.org/10.3390/ijms222111392

Śliwa, P., Śliwa, K., Sikora, E., Ogonowski, J., Oszmiański, J. and Nowicka, P., 2019. Incorporation of bioflavonoids from Bidens tripartite into micelles of non-ionic surfactants—Experimental and theoretical studies. Colloids and Surfaces B: Biointerfaces. 184: 110553. https://doi.org/10.1016/j.colsurfb.2019.110553

Suga, K., Kondo, D., Otsuka, Y., Okamoto, Y. and Umakoshi, H., 2016. Characterization of aqueous oleic acid/oleate dispersions by fluorescent probes and Raman spectroscopy. Langmuir. 32(30): 7606–7612. https://doi.org/10.1021/acs.langmuir.6b02257

Suliman, S.S., Othman, N., Mohamed Noah, N.F., Johari, K. and Ali, N., 2022. Stability of primary emulsion assisted with nanoparticle in emulsion liquid membrane process for zinc extraction. Materials Today: Proceedings. 65: 3081–3092. https://doi.org/10.1016/j.matpr.2022.05.532

Sun, D., Kang, S., Liu, C., Lu, Q., Cui, L. and Hu, B., 2016. Effect of zeta potential and particle size on the stability of SiO nanospheres as carrier for ultrasound imaging contrast agents. International Journal of Electrochemical Science. 11(10): 8520–8529. https://doi.org/10.20964/2016.10.30

Tyagi, A.K., Prasad, S., Yuan, W., Li, S. and Aggarwal, B.B., 2015. Identification of a novel compound (β-sesquiphellandrene) from turmeric (*Curcuma longa*) with anticancer potential: Comparison with curcumin. Investigational New Drugs. 33(6): 1175–1186. https://doi.org/10.1007/s10637-015-0296-5

Vinarov, Z., Dobreva, P. and Tcholakova, S., 2018. Effect of surfactant molecular structure on progesterone solubilization. Journal of Drug Delivery Science and Technology. 43: 44–49. https://doi.org/10.1016/j.jddst.2017.09.014

Wu, H., Liu, Z., Zhang, Y., Gao, B., Li, Y., He, X., *et al*. 2024. Chemical composition of turmeric (*Curcuma longa* L.) ethanol extract and its antimicrobial activities and free radical scavenging capacities. Foods. 13(10): 1550. https://doi.org/10.3390/foods13101550

Wu, J., Zhao, H., Xiao, D., Chuong, P.-H., He, J. and He, H., 2016. Mixed hemimicelles solid-phase extraction of cephalosporins in biological samples with ionic liquid-coated magnetic graphene oxide nanoparticles coupled with high-performance liquid chromatographic analysis. Journal of Chromatography A. 1454: 1–8. https://doi.org/10.1016/j.chroma.2016.05.071

Yamini, Y., Feizi, N. and Moradi, M., 2020. Surfactant-based extraction systems. In: Poole, C.F., editor. Handbooks in separation science, liquid–phase extraction. UK: Elsevier. pp. 209–239. https://doi.org/10.1016/B978-0-12-816911-7.00007-4

Yang, Q.-Q., Cheng, L.-Z., Zhang, T., Yaron, S., Jiang, H.-X., Sui, Z.-Q., *et al*. 2020. Phenolic profiles, antioxidant, and antiproliferative activities of turmeric (*Curcuma longa*). Industrial Crops and Products. 152: 112561. https://doi.org/10.1016/j.indcrop.2020.112561

Yusuf, H., Wijiani, N., Rahmawati, R.A., Primaharinastiti, R., Rijal, M.A.S. and Isadiartuti, D., 2021. Analytical method for the determination of curcumin entrapped in polymeric micellar powder using HPLC. Journal of Basic and Clinical Physiology and Pharmacology. 32(4): 867–873. https://doi.org/10.1515/jbcpp-2020-0491

Zarei, A.R., 2009. Spectrophotometric determination of trace amounts of furfural in water samples after mixed micelle-mediated extraction. Acta Chimica Slovenia. 7. Available from: https://acta-arhiv.chem-soc.si/56/56-2-322.pdf

Zhang, C., Yang, X., Dai, J., Liu, W., Yang, H. and Bai, Z., 2023. Efficient extraction of phenol from wastewater by ionic micro-emulsion method: Anionic and cationic. Chinese Journal of Chemical Engineering. 58: 137–145. https://doi.org/10.1016/j.cjche.2022.11.003

Zhang, W., Liu, X., Fan, H., Zhu, D., Wu, X., Huang, X., *et al*. 2016. Separation and purification of alkaloids from *Sophora flavescens* Ait. by focused microwave-assisted aqueous two-phase extraction coupled with reversed micellar extraction. Industrial Crops and Products. 86: 231–238. https://doi.org/10.1016/j.indcrop.2016.03.052

Ziyatdinova, G.K. and Budnikov, H.C., 2021. Micellar extraction of active components from spices and evaluation of the Ce(IV)-based reducing capacity of the extracts. Journal of Analytical Chemistry. 76(9): 1065–1070. https://doi.org/10.1134/S1061934821090124

Ziyatdinova, G., Ziganshina, E., Cong, P.N. and Budnikov, H., 2016. Ultrasound-assisted micellar extraction of phenolic antioxidants from spices and antioxidant properties of the extracts based on coulometric titration data. Analytical Methods. 8(39): 7150–7157. https://doi.org/10.1039/C6AY02112C